Theory of Polymer Brushes Grafted to Finite Surfaces

Agustín Santiago Andreu Artola, Ezequiel Rodolfo Soulé

Nanostructured Polymers Division, Institute of Materials Science (INTEMA) – National Research Council and University of Mar del Plata, Juan B. Justo 4302, Mar del Plata, Buenos Aires 7600, Argentina
Correspondence to: E. R. Soulé (E-mail: Ersoule@fi.mdp.edu.ar)

Received 27 September 2017; accepted 8 January 2018; published online 30 January 2018
DOI: 10.1002/polb.24577

ABSTRACT: In this work, a model based in strong-stretching theory for polymer brushes grafted to finite planar surfaces is developed and solved numerically for two geometries: stripe-like and disk-like surfaces. There is a single parameter, R^*_∞, which represents the ratio between the equilibrium brush height and the grafting surface size, that controls the behavior of the system. When R^*_∞ is large, the system behaves as if the polymer were grafted to a single line or point and the brush adopts a cylindrical or spherical shape. In the opposite extreme when it is small, the brush behaves as semi-infinite and can be described as a planar undeformed brush region and an edge region, and the line tension approaches a limiting value. In the intermediate case, a brush with non-uniform height and chain tilting is observed, with a shape and line tension depending on the value of R^*_∞. Relative stability of disk-shaped, stripe-shaped, and infinite lamellar micelles is analyzed based in this model. © 2018 Wiley Periodicals, Inc. J. Polym. Sci., Part B: Polym. Phys. **2018**, *56*, 663–672

KEYWORDS: finite-size effects; line tension polymer brush; self-consistent field theory; strong stretching

INTRODUCTION The physics of polymer brushes, that is, polymer layers adsorbed at one end to a surface, is of fundamental interest[1] in materials science and engineering. Polymer-functionalized solid surfaces,[2,3] stabilized or functionalized micro- or nano-colloidal particles,[4–8] nanostructures in block-copolymer systems,[9–11] are just a few examples of material systems where polymer brushes are present. A large volume of theoretical and simulation work have been reported in the literature, aimed to understand the equilibrium properties (equilibrium height, density profile) of polymer brushes.[12–26] Different theoretical approaches with different level of physical detail have been developed. The earlier approaches due to Alexander and de Gennes, were based in Flory theory. This approach is based in the asumptions that the chains are uniformly stretched and that the concentration is uniform throughout the brush, and they lead to the so-called scaling laws.[12–14] Despite its important simplifications, these theories can describe the overall properties of the brush fairly well. One important result of the scaling picture is that the thickness of the brush in equilibrium scales as $N^{3/(d+3)}$, where N is the number of Kuhn segments of the chain, and $d = 0$ for planar, 1 for cylindrical and 2 for spherical brushes.[19,27,28]

When a more detailed description or accurate calculations are required, scaling theories are not adequate. A more complex and precise description of polymer brushes is based in the self-consistent field theory (SCFT),[28–30] which describes the density distributions in a mesoscopic scale by using a mean-field approximation. There are more complex and exact theories, for example accounting for the effect of thermal fluctuations,[31] but the mean-field approximation works well in most cases and SCFT (and its variants) is the most widely theoretical framework used. The solution of the full SCFT is often not possible analytically, even for the simplest systems. Semenov,[15] and later Milner et al.[16–18] and independently Zhulina et al.,[26] developed a Strong-Stretching Theory (SST) that assumes that the chains are fully stretched, such that only the chain path that minimizes the free energy is relevant and fluctuations are unimportant. In these conditions the SCFT equations can be solved analytically for simple geometries. This theory predicts that the concentration profile inside the brush is parabolic.

The analysis of most of the previous works was restricted to simple geometries: infinite planes, cylinders, or spheres, such that the chain paths extend perpendicular to the grafting surface, and the problem becomes one dimensional. With the advances in nanoscience and nanotechnology in the last decades, the ability of nano-scale synthesis and processing had led to the emergence of systems where polymer brushes are not confined to infinite surfaces or simple geometries, and finite-size effects, that is the presence of an "edge," play a crucial role in the brush structure. That is the case of, to

mention a few examples, polymers grafted to nanopatterned surfaces,[3] finite lamellar micelles, ribbon-like or disk-like micelles in the case of block copolymers with one crystalline block,[22,32–35] platelet-like stabilized colloids,[8] etc. Despite its importance, only a few theoretical works have dealt with the case of brushes with edges, and all of them based in strong simplifications. Raphael and de Gennes considered the case of brushes in finite plates, using a simple Flory theory combined by a phenomenological Landau–Ginzburg free energy to describe the effect of the edge.[36] Gross et al. considered brushes in finite planes (stripe-like) and circles, in poor solvents, using scaling arguments and assuming *a priori* different configurations (e.g., cylindrical brush, planar brush, lateral micelles),[37] and Vilgis analyzed the case of a semi-infinite planar brush under compression, within a Flory approximation, where he considered that all chains extended between two fixed surfaces.[38] Williams and Fredrickson considered the case of disk-like micelles of block copolymers, by making the assumption that, at some distance from the surface, the chains paths adopted a radial configuration, which limits the treatment to the cases where the brush height is much bigger than the radius of the grafting surface.[22] With this model, they compared the relative stability of infinite lamellar and finite disk-like micelles, and found that the later are stable for certain range of parameter values.

In this work, planar brushes in a stripe-like and a disk-like surface will be considered, within the framework of Milner's SST. This theory is more accurate than Flory theories so the present model is expected to be more exact than the previous works; in addition, as the brush shape is not previously assumed nor constrained as in previous works, it is also more general, within the applicability of SST (for a discussion of the range of validity of SST see ref. 39). As SST can be solved analytically for the chain path, the model reduces to a system of ordinary differential equations, and with a proper non-dimensionalization there is only one parameter that determines the solution. The structure of the brush and its properties (equilibrium height and chain tilting, free energy, and line tension), are calculated in the whole parametric range, and limiting cases (where the chains are much smaller or much larger than the width of the grafting surface) are identified and compared to analytical solutions. Finally, relative stability of planar micelles with finite size and different shapes (stripe-like and disk-like) and infinite size is assessed with this model in terms of a dimensionless surface energy.

The paper is organized as follows: in the Model section, the model based in SST is presented. First, the case of infinite brush is considered, followed by the case of finite brushes and finally, the case of line and point brushes (which corresponds to the limit of very large chains) are presented. Results and discussion section presents the main results of the numerical solution of the model, and the analytical results corresponding to the limiting cases, divided into three subsections: brush structure, brush free energy, and relative stability in micellar systems. Finally, the conclusions are given in the Conclusions section.

MODEL

Infinite Brush

First, the case of an infinite brush will be briefly reviewed, as some of these results will be used for the finite brush. The polymer segments of a given chain are located along a curve $\mathbf{r}_{\text{chain}}(n)$, called the chain path. The variable n is the number of Kuhn segments comprised in a chain section that goes from the origin of the chain to a position $\mathbf{r}_{\text{chain}}$ along it. Following the strong stretching theory of Milner,[16–18] the free energy (in k_bT units) of a single chain with a given chain path can be calculated as:

$$F_{\text{chain},\mathbf{r}} = wv\int_0^N \phi dn + \frac{3}{2a^2}\int_0^N \left(\frac{d\mathbf{r}_{\text{chain}}}{dn}\right)^2 dn \tag{1}$$

where the first term accounts for excluded volume interactions, and the second term accounts for chain stretching. In that equation, ϕ is the volume fraction of polymer, w is the excluded volume parameter ($w > 0$), a is the Kuhn segment length, and N is the total number of Kuhn segments of a chain, and v is the volume of a chain segment. Note that the excluded volume interaction is usually considered in terms of $w\phi^2 dV$ (where V is the total volume), but in eq 1 the fact that $\phi_{\text{chain}} dV$ (where ϕ_{chain} is the volume fraction of a single chain) can be written as vdn was used.

In the strong stretching limit only the chain path that minimizes the free energy, $\mathbf{r}_{\text{eq}}$ is considered. This is obtained from the functional minimization of the chain free energy:

$$\frac{\delta F_{\text{chain},\mathbf{r}}}{\delta \mathbf{r}_{\text{chain}}} = \frac{\partial F_{\text{chain},\mathbf{r}}}{\partial \mathbf{r}_{\text{chain}}} - \nabla \cdot \frac{\partial F_{\text{chain},\mathbf{r}}}{\partial(\nabla \mathbf{r}_{\text{chain}})} = wv\frac{\partial \phi}{\partial \mathbf{r}_{\text{chain}}} - \frac{3}{a^2}\frac{\partial^2 \mathbf{r}_{\text{chain}}}{\partial n^2} = 0 \tag{2}$$

In the case of an infinite brush, $\mathbf{r}_{\text{eq}}(n)$ is a straight, vertical line. As discussed by Milner and others, for a chain whose end-segment is in a position r_N, and with no stretching in the free end ($dr_{\text{chain}}/dn = 0$ for $r = r_N$) this equation has a solution:

$$r_{\text{eq}} = r_N \sin\left(\frac{\pi}{2N} n\right) \tag{3}$$

Where r_{eq} is the position along the chain path. The concentration profile is parabolic,

$$\phi = A - Br^2 = A - \frac{3\pi^2}{8a^2 wvN^2} r^2 \tag{4}$$

Where A and B are constants and r the direction perpendicular to the grafting surface. The value of B is determined from the boundary conditions and it is as shown in eq 4.

The concentration profile must satisfy the following constraint:

$$vN = \frac{1}{\sigma}\int_0^R \phi dy \tag{5}$$

where σ is the number of chains grafted per unit area and R the brush height. Both sides of this equation represent the total volume occupied by one polymer chain; in the left-hand side it is calculated from the number of chains present in the system, and in the right-hand side, from the concentration profile. Inserting eq 4 in eq 5:

$$A = \frac{v\sigma N}{R} + \frac{\pi^2}{8a^2 wvN^2}R^2 \tag{6}$$

When the concentration profile is introduced in the free energy:

$$F_{\text{chain},\mathbf{r}_{\text{eq}}} = wv\int_0^N \left(A - B\left(r_N \sin\left(\frac{\pi n}{2N}\right)\right)^2\right)dn + \frac{3\pi r_N}{8a^2 N}\int_0^N \left(\cos\left(\frac{\pi n}{2N}\right)\right)^2 dn \tag{7}$$

If B is replaced by its expression given in eq 4:

$$F_{\text{chain},\mathbf{r}_{\text{eq}}} = \frac{wv}{2}\int_0^N A dn + \frac{3\pi^2 r_N^2}{8a^2N^2}\int_0^N \left[\left(\cos\left(\frac{\pi n}{2N}\right)\right)^2 - \left(\sin\left(\frac{\pi n}{2N}\right)\right)^2\right]dn = wvNA \tag{8}$$

Obtaining the remarkable result that the free energy is independent of the end-segment position r_N. Replacing A, the equilibrium height of an infinite brush can be obtained from the minimization of the free energy:

$$R_{\text{eq},\infty} = \left(\frac{3N\sigma\tilde{v}}{2B}\right)^{1/3} = \left(\frac{4a^2 wN^3\sigma v^2}{\pi^2}\right)^{\frac{1}{3}} \tag{9}$$

With this result, the concentration profile can be re-written as:

$$\phi = B\left(R_{\text{eq},\infty}{}^2 - r^2\right) \tag{10}$$

And the free energy can be calculated as:

$$F_{\text{chain,eq}} = wvNBR_{\text{eq}}{}^2 \tag{11}$$

Note that the "∞" index has been removed, as this expression is actually valid for any geometry as long as $A = BR_{\text{eq}}{}^2$, that is, when the concentration is parabolic and drops to zero at the endpoint of the chain, regardless the shape of the chain path.

Finite Brushes: Edge Effects

The case of a polymer brush attached to a surface which is finite in one direction and infinite in the other, that is, a "stripe" brush, is considered first. Figure 1 shows a schematic of the system under consideration. The surface dimensions are $2L$ in the x direction Z in the z direction (perpendicular to the xy plane), with Z large enough such that it is effectively infinite in that direction. The origin $x = 0$ is at the center of the brush, and the edge corresponds to $x = L$. Close to the border, the chains tilt and curve outwards, but a simplified scenario with straight chain paths will be considered, as shown in Figure 1.

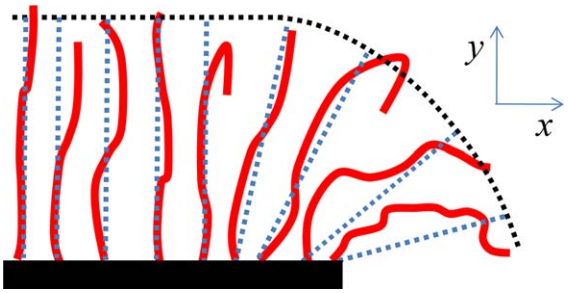

FIGURE 1 Schematics of the edge of a finite planar brush. Polymer chains are shown as full red lines, with the corresponding chain paths shown as dotted blue lines. The simplification that the chain paths are straight is used, although in real systems they might be curved as they tilt outwards. The black dotted line represents the outer limit of the brush. [Color figure can be viewed at wileyonlinelibrary.com]

The coordinates used to describe a chain are shown in Figure 2. The position of the grafting point of the chain is x_0, S and H are the total lateral displacement and height of the chain, such that the position of the chain end is (x_0+S, H), and the total length of the chain path is $R=(S^2+H^2)^{1/2}$. Note that H, S, and R are functions of x_0. The position of a chain segment is given by $(x_n = x_0+y_nS/H, y_n)$, and its distance to the grafting point is $r_n = y_n(1 + S^2/H^2)^{1/2}$.

Ball et al.[21] have shown that the parabolic concentration profile is only valid for planar geometry, while in curved surfaces this would lead to the existence of a zone with an unphysical negative concentration of chain free ends. Consequently, there is an "exclusion zone" where the concentration of chain ends is zero, and the concentration profile deviates from the parabolic shape. This is also the case in a finite brush, where the chains are tilted and the brush is curved outwards. In this case, the chain paths cannot be explicitly solved and eq 11 would, strictly, not be valid. Nevertheless, as the authors show in the same paper, the free energy is remarkably well reproduced when a parabolic profile is used; they actually use it in another work where they

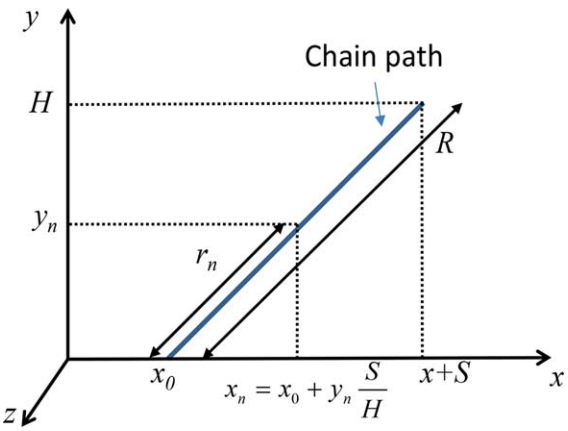

FIGURE 2 Definition of coordinates and variables used in the model. [Color figure can be viewed at wileyonlinelibrary.com]

analyze curved brushes.[40] Consequently, considering that the results presented in this work depend on the free energy and characterizing the concentration profiles or the segment distribution is not the main goal, the parabolic concentration profile (that allows explicit solutions for the chain paths) will be used. With this consideration, eqs 1 through 8 are valid for the finite brush, and the constraint imposed to the concentration profile (derived in the Appendix) is given by:

$$\sigma v N = \int_0^H \phi \left[1 + \frac{y_n}{H} S' - S \frac{y_n}{H^2} H'\right] dy_n \tag{12}$$

where the primes denotes derivatives (with respect to x_0). The equilibrium structure of the brush is given by the profiles $S(x_0)$ and $H(x_0)$ that minimize the free energy, subjected to the constraint given by eq 12. The problem can be simplified as follows. As the free energy is proportional to A (eq 8), the value of A has to be minimum. This is the case when the concentration drops to zero at the end point of the brush, so eq 11 is valid in this case too.[40] Considering, in addition, that $r_n/R = y_n/H$, the problem reduces to minimizing the total brush free energy, which, using eq 11, is:

$$F = 2\sigma Z \int_0^L F_{\text{chain,eq}} dx_0 = 2wvN\sigma BZ \int_0^L \left(H^2 + S^2\right) dx_0 \tag{13}$$

subject to the constraint:

$$\frac{\sigma v N}{B} = \left(S^2 + H^2\right)\left[\frac{2}{3}H + \frac{1}{4}HS' - \frac{1}{4}SH'\right] \tag{14}$$

The case of a brush attached to a circular surface, that is a "disk" brush, was also considered. The diameter of the disk is D. In this case the equations are:

$$F = \sigma\pi \int_0^{D/2} x_0 F_{\text{chain,eq}} dx_0 = \pi wvN\sigma B \int_0^{D/2} x_0 \left(H^2 + S^2\right) dx_0 \tag{15}$$

Subject to the constraint (derived in the Appendix):

$$\begin{aligned} x_0 \frac{\sigma v N}{B} = {} & x_0 \left(S^2 + H^2\right)\left[\frac{2}{3}H + \frac{1}{4}HS' - \frac{1}{4}SH'\right] \\ & + S\left(S^2 + H^2\right)\left[\frac{1}{4}H + \frac{2}{15}HS' - \frac{2}{15}SH'\right] \end{aligned} \tag{16}$$

The problem was solved by using the method of Lagrange multipliers for constrained minimization. The differential equations were solved by a finite-differences method. The constraint equation (eq 14 or 16) is first order, so it requires one boundary condition. Functional minimization of the free energy, after elimination of Lagrange multipliers, leads to a second-order equation and requires two boundary conditions. In principle, only the symmetry conditions $S = 0$ and $dH/dx = 0$ at the center of the brush ($x_0 = 0$) are imposed. As the value H_{edge} is not given by any external condition, the system of equations was solved for different values of H_{edge}; the one that minimizes the free energy corresponds to the equilibrium value. It was found that the free energy decreases as H_{edge} decreases, such that the minimum corresponds to a negative value of H_{edge}. In this work, only the case of non-negative H_{edge} is considered, corresponding to a physical system with an impenetrable surface at $y = 0$, for example when the solid substrate extends beyond the grafting area of the brush, or to the case of thin planar micelles (where the surface at $y = 0$ is a symmetry plane). With this restriction, the free energy is minimized for $H_{\text{edge}} = 0$.

Brushes in Infinitesimal Surfaces

A third case is considered, that corresponds to the limiting case when chain length much larger that L or D; in this case the stripe brush behaves as if the chains were attached to a line, and the disk brush as if the chains were attached to a point; in both cases they will extend outwards radially.

In the case of a "line" brush, the chain-volume constraint is:

$$\frac{p}{Z}\tilde{v}N = 2\pi \int_0^R \phi r dr \tag{17}$$

where p is the total number of polymer chains in the brush, such that p/Z is the number of chains per unit length of the brush. In terms of the variables considered for the stripe brush, p/Z is equivalent to $2\sigma L$. Minimizing the free energy given by eq 11, subjected to that constraint and using this equivalence, the equilibrium chain length is obtained:

$$R_{\text{eq,line}} = \left(\frac{8L\sigma vN}{\pi B}\right)^{\frac{1}{4}} = \left(\frac{64L\sigma v^2 wa^2 N^3}{3\pi^3}\right)^{\frac{1}{4}} \tag{18}$$

In the case of a "point" brush, the constraint is:

$$pvN = 2\pi \int_0^R \phi r dr \tag{19}$$

Where $p = \sigma\pi D^2/4$. Minimization of the free energy in this case leads to the equilibrium length:

$$R_{\text{eq,point}} = \left(\frac{15}{16}\frac{D^2\sigma vN}{B}\right)^{\frac{1}{5}} = \left(\frac{5D^2\sigma v^2 wa^2 N^3}{2\pi^2}\right)^{\frac{1}{5}} \tag{20}$$

Dimensionless Variables and Parameters

The characteristic length used to non-dimensionalize all spatial variables is $l = L$ for the stripe, and $l = D/2$ for the disk. With this non-dimensionalization, the solution of the equilibrium equations depends on a single dimensionless group, $\sigma vN/Bl3$. The equilibrium solutions will be described in terms of the ratio between the equilibrium height of an infinite brush and the surface length:

$$R_\infty{}^* = \frac{R_{\text{eq},\infty}}{l} = \left(\frac{3\sigma vN}{2Bl^3}\right)^{\frac{1}{3}} \tag{21}$$

The equilibrium size of a line brush and point brush is given in eqs 22 and 23 in terms of this parameter:

$$R_{\mathrm{eq,line}} = \left(\frac{16}{3\pi} {R_\infty}^{*-3}\right)^{\frac{1}{4}} L \tag{22}$$

$$R_{\mathrm{eq,point}} = \frac{1}{2}\left(\frac{20}{8} {R_\infty}^{*-2}\right)^{\frac{2}{5}} D \tag{23}$$

The dimensionless free energy is defined in terms of the free energy of an infinite brush as:

$$F^* = \frac{2F}{2wvN\sigma\theta B {R_{\mathrm{eq}}}^2} \tag{24}$$

where θ is the area of the grafting surface. The dimensionless free energy for an infinite brush is then 1, and for the cases of line and point brushes it reduces to the following analytical expressions:

$${F^*}_{\mathrm{line}} = 2\left(\frac{4}{3\pi}\right)^{\frac{1}{2}} {R_\infty}^{*-\frac{1}{2}} \tag{25}$$

$${F^*}_{\mathrm{point}} = \left(\frac{5}{8}\right)^{\frac{2}{5}} 2^{\frac{4}{5}} {R_\infty}^{**\frac{-4}{5}} \tag{26}$$

Finally, the line tension λ, which is the (negative) excess energy per unit length introduced by the presence of the edge, is calculated from eq 27:

$$F = F_\infty - \lambda C \tag{27}$$

Where C is the length of the edge: $C_{\mathrm{stripe}} = 2Z$ and $C_{\mathrm{disk}} = \pi D$. A dimensionless line tension can be defined and calculated by eq 28:

$$\frac{\lambda}{wvN\sigma B {R_{\mathrm{eq}}}^3} = \lambda^* = \frac{1 - F^*}{k {R_\infty}^*} \tag{28}$$

Where $k = 1$ for stripes and $k = 2$ for disks.

RESULTS AND DISCUSSION

Structure

The equilibrium equations were solved in a broad range of R^*_∞, observing two limiting cases: for very large R^*_∞ (corresponding to $R_{\mathrm{eq},\infty} \gg l$), the chains are much larger than the grafting surface and they behave as line brush or point brush. In the opposite extreme, when $R_{\mathrm{eq},\infty}$ is small compared to l, the chains are much smaller than the grafting surface and the brush behaves as semi-infinite, composed by a region of undistorted brush (vertical chain paths), and an "edge region," with a (normalized) shape and structure that is independent of R^*_∞. Similar regimes where identified and considered by Gross et al.,[37] although in that work they are treated within a simplified scaling theory, and intermediate regimes are not considered.

Figures 3 and 4 show the structure of the stripe brush, the case of the disk brush is similar so it is not shown. Figure 3 shows the shape of the stripe brush as a function of R^*_∞. The coordinates of the brush outer limit, that is H versus x_0+S, are plotted. Figure 3(a) shows the case of large R^*_∞, where the semi-circular shape limit is observed; while Figure 3(b) shows the opposite case of small R^*_∞, where the semi-infinite behavior can be observed. Note that in Figure 3(b) the x-coordinate is shifted (so that the 0 is placed at the edge), and re-scaled with respect to R_∞, so that the limit of R^*_∞-independent shape is observed. For large R^*_∞, the disk brush has the same circular shape, but the value of R_{eq} is smaller than for the stripe brush. For small R^*_∞, where the curvature of the grafting surface becomes negligible, the brush structure is the same for both geometries.

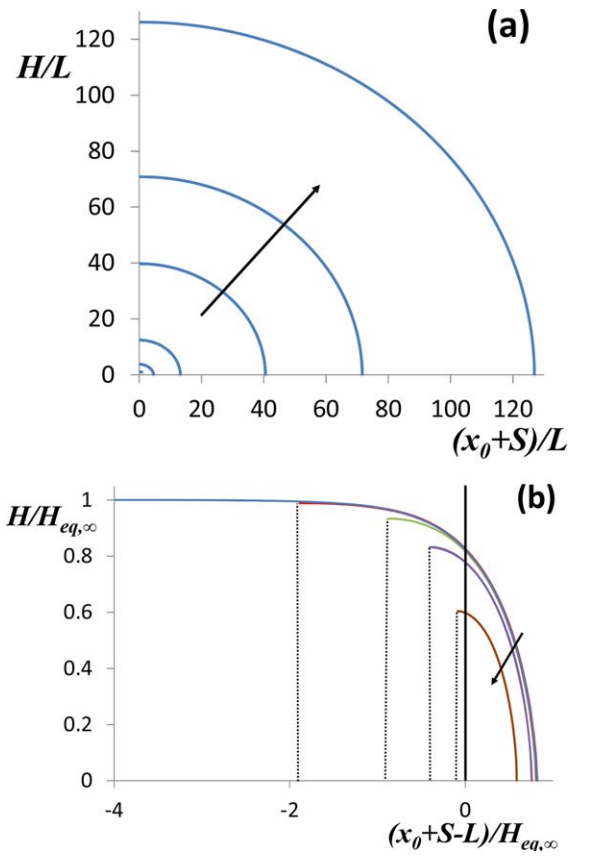

FIGURE 3 Shape of the brush for different values of the parameter R^*_∞. (a) $R^*_\infty = 1.14$, 5.31, 24.6, 114, 246, 531, and (b) $R^*_\infty = 0.0531$, 0.531, 1.14, 2.46, 11.4, increasing in the direction of the arrow. Note the different axis in each figures. [Color figure can be viewed at wileyonlinelibrary.com]

Figure 4(a–c) shows the chain paths (in the upper panel), and the profiles of H, S, and R as a function of x_0 (lower panel), for the cases of large [Fig. 4(a)], intermediate [Fig. 4(b)], and small [Fig. 4(c)] R^*_∞, in a stripe brush (for disk brushes they are qualitatively similar). Figure 4(a) shows the line brush regime, where R is constant and the profiles H versus x_0 and S versus x_0 approach a cosine and sine function respectively; for a disk brush, H and S approach$(1–x)^2$ and $(1–(1–x)^2)^{1/2}$. In the intermediate regime, Figure 4(b), the shape is not circular, but the brush is distorted everywhere, with a non-zero gradient of S and an equilibrium chain length close to, but smaller than $R_{\mathrm{eq},\infty}$. In Figure 4(c),

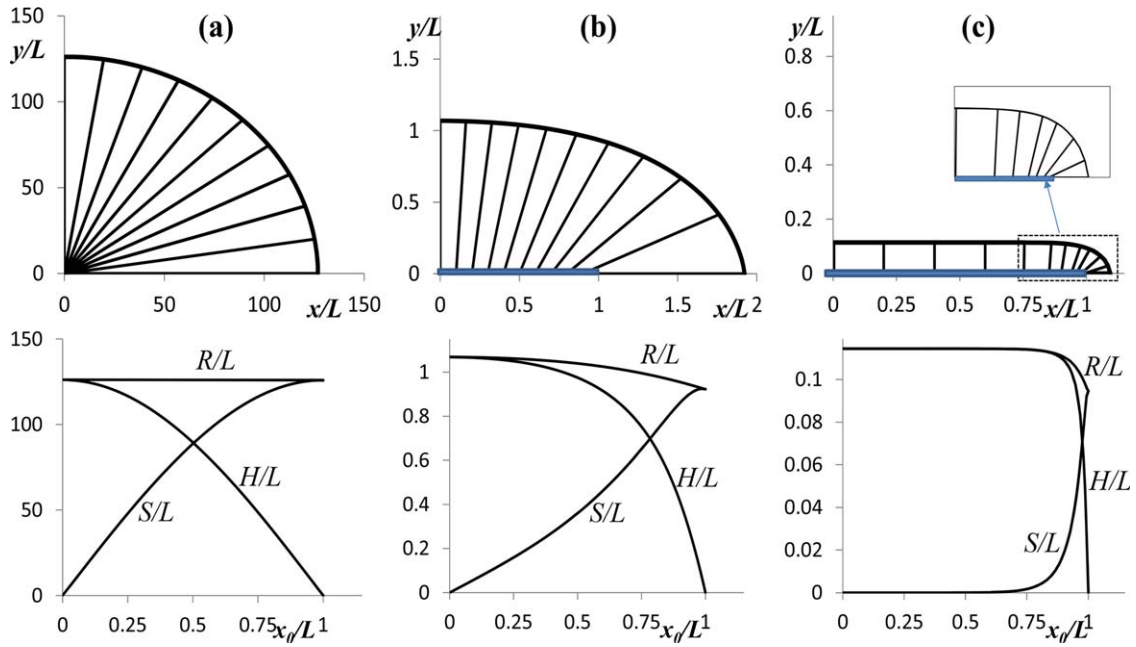

FIGURE 4 Chain paths (upper panel), and profiles of H, S, and R (lower panel) in different brush regimes. In the upper panel the grafting surface is drawn in blue color. (a) $R^*_\infty = 531$, corresponding to the cylindrical brush polymer regime, (b) $R^*_\infty = 1.14$, corresponding to the intermediate regime, (c) $R^*_\infty = 0.114$, corresponding to the semi-infinite brush regime. The inset shows the edge region. Note that each figure has a different scale. [Color figure can be viewed at wileyonlinelibrary.com]

the regime of semi-infinite brush is shown, where the chain paths are mostly vertical, with $H = R_{eq,\infty}$, and only close to the edge they tilt outwards with decreasing H and non-zero S and S'. The size of this "edge region" can be observed to be of about $2R^*_\infty$. Note that the semi-infinite brush limit breaks down when R^*_∞ is about 0.5, that is, when the whole brush size equals the edge size.

Figure 5(a) shows the values of $R/R_{eq,\infty}$ at the center of the brush, at $x = L$, and its mean value, as a function of R^*_∞. The limiting values are, respectively, 1, 0.83, and 1 as R^*_∞ goes to zero, (semi-infinite brush), and the three curves converge, approaching zero, in the regime of large R^*_∞. Both the stripe and disk brush behave the same, but the disk brush has a smaller value of $R/R_{eq,\infty}$, it deviates from the semi-infinite behavior at smaller values of R^*_∞, and approaches to 0 faster than the stripe brush, as expected due to the larger curvature of the surface. Figure 5(b) shows R/L as a function of R^*_∞ in double log scale, where the two limiting behaviors given by eqs 22 and 23 are observed.

The extension of the chain paths R, as expected, is smaller in the edge than in the center, due to the extra free volume available to the chains. But it is worth to note that the decrease in chain size introduced by the edge is relatively small, the lowest value of $R(x = L)/R(x = 0)$ is 0.83. Consequently, the presence of the edge does not compromise the validity of the strong stretching approximation.

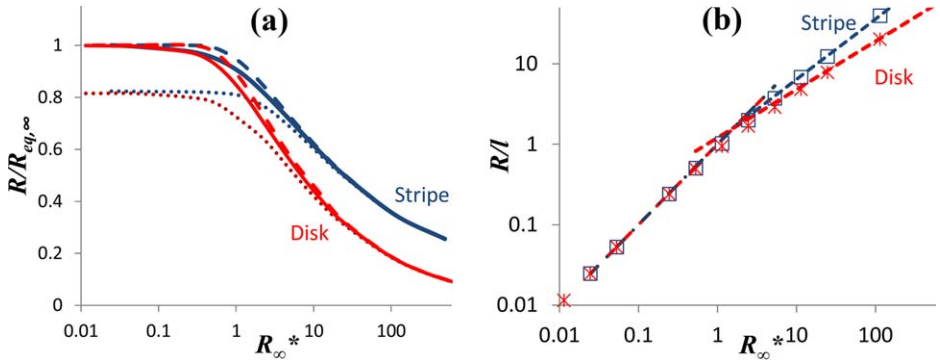

FIGURE 5 Some representative values of R as a function of R^*_∞. (a) R/R^*_∞ at $x = 0$ (dashed line), $x = L$ (dotted line), and mean value of the brush (full line). (b) Mean value of R/l of the finite brush (crosses), and of an infinite brush and a cylindrical brush polymer (dotted lines). [Color figure can be viewed at wileyonlinelibrary.com]

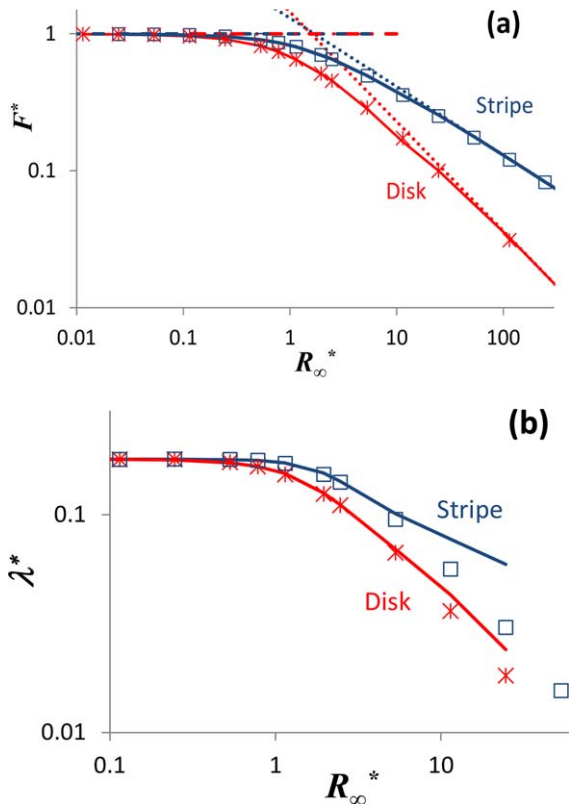

FIGURE 6 (a) Free energy of the brush as a function of R^*_∞, (b) line tension, as a function of R^*_∞. The squares and stars are the calculated values, the dotted lines correspond to the limits of infinite and cylindrical brush polymer (eqs 25, 26, and 28), the dashed line is the limit of infinite brush, and the full line is the approximation given by eqs 32 and 34. [Color figure can be viewed at wileyonlinelibrary.com]

Free Energy

Figure 6(a,b) shows the free energy and the line tension as a function of R^*_∞. The free energy of the disk-brush is smaller than the stripe brush. This is expected due to the fact that the disk has a larger curvature, or equivalently a larger perimeter, so edge effects (which decrease the free energy) are more significant. For R^*_∞ close to zero, the free energy approaches 1, the value that corresponds to an infinite brush. As R^*_∞ increases, edge effect become increasingly more significant, lowering the free energy, until the line- and point-brush limits (eqs 25 and 26) are approached for large R^*_∞. The limiting behaviors of small and large R^*_∞ are shown in Figure 6(a), as well as an approximating function constructed by combining these limiting cases (this is explained in the following section).

The line tension reaches a limiting constant value, which is $\lambda^*_\infty = 0.18$, as R^*_∞ goes to zero. This is expected considering that the structure of the brush edge becomes independent on R^*_∞ in this range. The line tension starts deviating significantly from λ^*_∞ at a value of R^*_∞ close to 0.5, that is when the size of the edge equals the size of the brush, as explained before (although there is a difference between stripe- and disk-brushes that will be discussed in the following paragraph).

An interesting observation, is that the line tension of the disk-brush is smaller than the stripe brush (as a consequence it starts deviating from the low R^*_∞ regime at smaller values of R^*_∞ than the stripe brush, as shown in Fig. 6). This seems to contradict the previous affirmation that edge effects are more significant in the disk-brush due to its higher curvature. Nevertheless, it has to be taken into account that the edge effect on the free energy arises from the product between the line tension and the perimeter/area ratio, which is $1/L$ for stripes and $2/L$ for disks, so there is no such contradiction. The fact that a disk brush seems to deviate from the semi-infinite regime for smaller values of R^*_∞, can be understood considering that when the size of the brush approaches the edge penetration length, the curvature of the grafting surface across the edge region is significant; this affects the structure of the brush in the edge region and consequently the line tension.

Application to Crystalline-Core Lamellar Micelles

As aforementioned, one physical system that can be represented as a finite brush is the case of lamellar micelles of finite size. This type of micelles can be found in a block copolymer (BCP) system with one crystalline block. In this section, the relative stability of different micelles (disks, stripes, infinite lamellas) in a BCP with a crystalline block will be estimated with a simplified model, using the results obtained for finite brushes. Although Williams and Fredrickson calculated a phase diagram including disk-like micelles and infinite lamellas (among other geometries),[22] to our knowledge a theoretical analysis of the relative stability of this three geometries has not been performed before.

Assuming that there are no free BCP chains (i.e., all the BCP molecules are forming part of the micelles), the total number of polymer molecules can be related to the number of micelles as:

$$P = m\sigma\theta \tag{29}$$

Where P is the total number of BCP molecules and m the number of micelles; θ in this case is the area of the micelle (monodispesity in micelle size is assumed). Neglecting the translation entropy of the micelles, the free energy of the micellar system is:

$$F_T = m(F_{brush} + \gamma C d) + F_{crys} + F_{int} \tag{30}$$

Where F_{crys} is the free energy of the crystalline core and F_{int} is the free energy of the interface between the micelle core and the brush; these two terms are considered independent of the micelle configuration. The free energy of the micelle corona is represented as F_{brush}, and corresponds to the energy of a stripe or a disk brush. The surface energy of the lateral surface of the micelle is γ and d is the thickness (Cd is the lateral area). Note that γ corresponds to an interface between the lateral surface of the crystalline core and the

solvent and it is different from the energy of the core/corona interface. It can also be anisotropic and depend on curvature, which would favor polygonal over disk-like micelles, but this effect is beyond the scope of the present analysis.

The dimensionless free energy per unit volume of the micelle system can be defined and calculated as:

$$\frac{Nv}{\phi_{BCP}}\frac{F_T}{2VwvBNR_{eq}{}^2}=\left(\frac{F_{brush}}{2wvBN\sigma\theta R_{eq}{}^2}+\frac{\gamma d}{2wvBN\sigma R_{eq}{}^3}kR_\infty{}^*\right)+\ldots \tag{31}$$

where V is the total volume of the system (BCP + solvent), ϕ_{BCP} the volume fraction of BCP in the system, and k, as before, is 1 for stripes and 2 for disks. The terms that do not depend on the micelle structure are not shown. Note that, in the real case the variables d and σ are not independent, and there is an extra "chain folding" energy in the crystalline phase that depends on those variables, but this effect is neglected in this simplified analysis.

The free energy of the micelles, eq 31, is minimized with respect to R^*_∞, to find the equilibrium size of the micelle (which is proportional to $R^*_\infty{}^{-1}$) and the equilibrium free energy of the micellar system as a function of the dimensionless surface energy, defined as $\gamma^*= \gamma d/wvBN\sigma R_{eq}{}^3$. Note that this dimensionless free energy includes the effect of both the surface tension and the micelle core thickness, so the relative size of the crystalline block is included in this parameter. The minimization of eq 31 is not numerically simple, as the dependence of the free energy on R^*_∞, is implicit and it is given through the functional minimization of F_{brush}, as discussed in the previous sections. To simplify the calculations, the dimensionless brush free energy for both geometries was fitted with arbitrary analytical functions which are explicit in R^*_∞. These functions were constructed by fitting the line tension for relatively small values of R^*_∞ (where it does not deviates significantly from 1), and combining this expression with the one corresponding to line- or point- brushes, as follows:

$$F^*{}_{stripe}=\left[1-\lambda_{stripe}{}^*(R_\infty{}^*)R_\infty{}^*\right]\left(1-\frac{2}{\pi}\arctan\left(\frac{R_\infty{}^*}{6.59}\right)^{3.184}\right)+\frac{2}{\pi}\arctan\left(\frac{R_\infty{}^*}{6.59}\right)^{3.184}F^*{}_{line} \tag{32a}$$

$$\lambda_{stripe}{}^*(R_\infty{}^*)=\lambda_\infty{}^*\exp\left[-\frac{1}{2.613R_\infty{}^{*-0.333}+34.98R_\infty{}^{*-2.992}}\right] \tag{32b}$$

$$F^*{}_{disk}=\left[1-2\lambda_{disk}{}^*(R_\infty{}^*)R_\infty{}^*\right]\left(1-\frac{2}{\pi}\arctan\left(\frac{R_\infty{}^*}{7.476}\right)^{2.979}\right)+\frac{2}{\pi}\arctan\left(\frac{R_\infty{}^*}{7.476}\right)^{2.979}F^*{}_{point} \tag{33a}$$

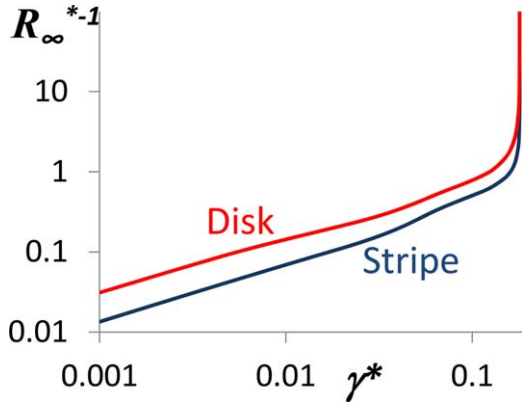

FIGURE 7 Dimensionless size of disk-like and stripe-like micelles as a function of the dimensionless surface energy. [Color figure can be viewed at wileyonlinelibrary.com]

$$\lambda_{diks}{}^*(R_\infty{}^*)=\lambda_\infty{}^*\exp\left[-\frac{1}{(2.658R_\infty{}^{*-0.634}+21.45R_\infty{}^{*-2.954})^{3/2}}\right] \tag{33b}$$

Equations 32 and 34 are shown in Figure 6(a,b) along with the calculated values of free energy and line tension, it can be seen that the fitting of the free energy is very good in the whole range of R^*_∞. Special care was taken in the region of small R^*_∞, that is critical for assessing the micelle stability. Note that the fitting of the line tension starts deviating from the calculated values at about $R^*_\infty = 10$, but at this point the term corresponding to line or point brushes has most of the weight in the free energy fitting.

The approximated expressions given by eqs 32a and 33a for the brush free energy can be introduced in eq 31, which now becomes explicit in R^*_∞ and can be easily minimized. Figure 7 shows the equilibrium value of $R^*_\infty{}^{-1}$ as a function of γ^*. It can be seen that it increases with γ^* and diverges when $\gamma^* = \lambda_\infty{}^*$. This can be understood considering that both the effect of the line tension and the surface energy are proportional to R^*_∞, that is, the free energy of the micellar system can be written as:

$$F_T{}^*=F^*{}_{brush,\infty}+[\gamma^*-\lambda^*(R_\infty{}^*)]kR_\infty{}^* \tag{34}$$

so the line tension will always be larger than the surface energy for a minimum at finite R^*_∞, if the surface energy is larger, the minimum is at $R^*_\infty = 0$ (infinite lamellar micelle).

Figure 8 shows the difference in free energy between the stripe- and disk-like micellar system, ΔF_T, as a function of γ^*. It can be seen that stripe micelles are stable for $\gamma^*>0.155$ and disk micelles for $\gamma^*<0.155$. Although it should be noted that the free energy difference between the two types of micelles is relatively small, so consideration of some neglected effects (particularly the anisotropy in the surface tension of the crystalline phase), would modify the calculated range of stability for the stripe micelle phase. If the surface tension depends on curvature, or on crystallographic

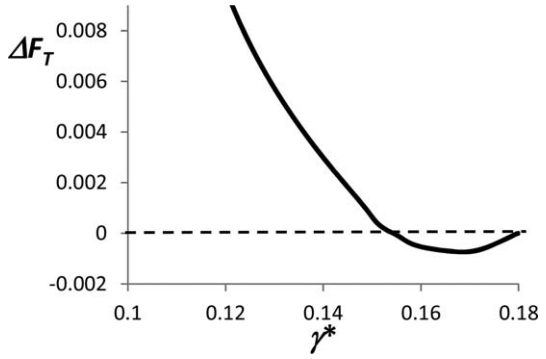

FIGURE 8 Free energy difference between stripe-like and disk-like micelles.

orientation such that faceted micelles are formed, this would lead to a higher surface energy for the disks micelles, increasing the range of stability of the stripe micelles.

CONCLUSIONS

A theory for a polymer brush grafted to a finite substrate, based in Milner parabolic strong-stretching theory, was developed. Disk-like and stripe-like geometries were considered. A single dimensionless parameter, R^*_∞, which is the ratio between the equilibrium height of an infinite-brush and the size of the grafting surface, controls the structure and thermodynamics of the brush.

The model was solved in a broad range of R^*_∞, such that limiting behaviors were observed. For small R^*_∞, the brush behaves as semi-infinite, such that the chain paths are perpendicular to the substrate everywhere except in a region close to the edge where they tilt outwards. The structure of this region becomes independent of R^*_∞ in this regime. For large R^*_∞, the line brush and point brushes limits are observed for the stripe and disk cases respectively; in this regime the chain paths behaves as if they were grafted to a line or a point, and extend outwards radially. In the intermediate regime, a deformed, non-uniform planar brush is observed, where the chains are significantly tilted everywhere, and the tilting increases as the edge is approached.

The dimensionless line tension was also evaluated and a limiting value of $\lambda_\infty{}^* = 0.18$ was approached as $R_\infty{}^*$ goes to zero. The penetration length of the edge is found to be about R^*_∞. The edge of a stripe brush, to a good approximation, can be considered to be in the low-R^*_∞ regime for $R^*_\infty < 0.5$, while for disk brushes, due to the curvature of the grafting surface, deviations from this regime are observed for smaller R^*_∞.

A simple model for micellar suspensions of block copolymer micelles with a crystalline core was constructed, and the relative stability of disk- and stripe-like micelles was assessed with this model. When the dimensionless surface energy of the lateral surface of the micelle is higher than the dimensionless line tension, infinite lamellar micelles are stable, while stripe micelles are stable when the surface energy is close but smaller than the line tension, and disk-like micelles are stable for smaller values of surface energy.

APPENDIX: DERIVATION OF THE CHAIN VOLUME CONSTRAINT

In this appendix, the constraints to the free-energy functional minimization, given by the consistency between the polymer composition profile and the total volume of polymer molecules, eqs 14 and 16, are derived. A differential volume, bounded between two chains located at x_0 and $x_0 + \mathrm{d}x_0$, is considered, as shown in Figure 9. The transversal area of this differential volume is a parallelogram can be calculated as:

$$d\Lambda = dx_\mathrm{n} dy \tag{A1}$$

So an expression for dx_n is needed.
As shown previously in the Finite brushes: edge effects section, x_n can be calculated as:

$$x_\mathrm{n} = x_0 + y_\mathrm{n}\frac{S}{H} \tag{A2}$$

So, considering that both S and H are functions of x_0, the differential is:

$$dx_\mathrm{n} = dx_0 + y_\mathrm{n}\left(\frac{S+dS}{H+dH} - \frac{S}{H}\right) \tag{A3}$$

Considering a Taylor expansion, and leaving only first-order terms:

$$\begin{aligned} dx_\mathrm{n} &= dx_0 + y_\mathrm{n}\left(\frac{dS}{H} - \frac{S}{H^2}dH\right) \\ &= dx_0\left(1 + \frac{y_\mathrm{n}}{H}\frac{dS}{dx_0} - \frac{Sy_\mathrm{n}}{H^2}\frac{dH}{dx_0}\right) \end{aligned} \tag{A4}$$

Combining eqs A1 and A4, for a stripe brush:

$$dV = Z\left(1 + \frac{y_\mathrm{n}}{H}\frac{dS}{dx_0} - \frac{Sy_\mathrm{n}}{H^2}\frac{dH}{dx_0}\right)dydx_0 \tag{A5}$$

Which leads to eq 12 for the number of chains per unit length in x_0. For a disk brush:

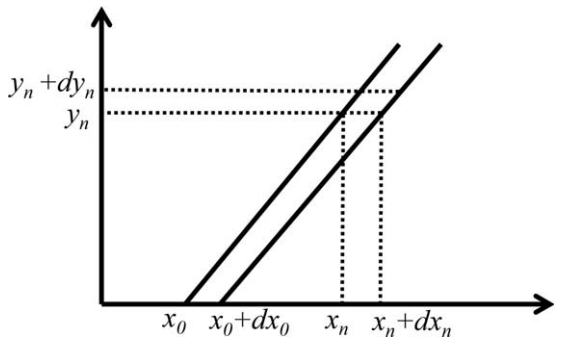

FIGURE 9 Representation of the differential volume used to calculate the total volume of a polymer chain.

$$dV = 2\pi\left(x_0 + y_n\frac{S}{H}\right)\left(1 + \frac{y_n}{H}\frac{dS}{dx_0} - \frac{Sy_n}{H^2}\frac{dH}{dx_0}\right)dydx_0 \quad \text{(A6)}$$

Which leads to

$$\begin{aligned} 2\pi\sigma\nu N x_0 dx_0 &= \int_0^H \phi dV \\ &= 2\pi\int_0^H \phi\left(x_0 + y_n\frac{S}{H}\right)\left(1 + \frac{y_n}{H}\frac{dS}{dx_0} - \frac{Sy_n}{H^2}\frac{dH}{dx_0}\right)dx_0 dy_n \end{aligned} \quad \text{(A7)}$$

and, after integration, to eq 16.

ACKNOWLEDGMENTS

This work was partially supported by the National Research Council (CONICET) and the National Agency for Promotion of Science and Technology (ANPCyT).

REFERENCES AND NOTES

1 B. Zhao, W. Brittain, *J. Prog. Polym. Sci.* **2000**, *25*, 677.

2 R. Barbey, L. Lavanant, D. Paripovic, N. Schuwer, C. Sugnaux, S. Tugulu, H.-A. Klok, *Chem. Rev.* **2009**, *109*, 5437.

3 A. G. Koutsioubas, A. G. Vanakaras, **2008**, *24*, 13717.

4 J. Kalb, D. Dukes, S. K. Kumar, R. S. Hoy, G. S. Grest, *Soft Matter* **2011**, *7*, 1418.

5 D. M. Trombly, V. Ganesan, *J. Chem. Phys.* **2010**, *133*, 154904.

6 X.-Q. Zhang, M. Chen, R. Lam, X. Xu, E. Osawa, D. Ho, *ACS Nano* **2009**, *3*, 2609.

7 V. Ganesan, C. J. Ellison, V. Pryamitsyn, *Soft Matter* **2010**, *6*, 4010.

8 A. Kirillova, G. Stoychev, L. Ionov, K.-J. Eichhorn, M. Malanin, A. Synytska, *Appl. Mater. Interfaces* **2015**, *7*, 21218.

9 Y. Shao, P. Aizhao, H. Ling, *J. Colloid Interface Sci.* **2014**, *425*, 5.

10 R. Karnik, F. Gu, P. Basto, C. Cannizzaro, L. Dean, W. Kyei-Manu, R. Langer, O. C. Farokhzad, *Nano Lett.* **2008**, *8*, 2906.

11 K. Letchford, H. Burt, *Eur. J. Pharm. Biopharm.* **2007**, *65*, 259.

12 S. Alexander, *J. Phys.* **1977**, *38*, 977.

13 P. G. de Gennes, **1980**, *1075*, 1069.

14 P. G. de Gennes, *Adv. Colloid Interface Sci.* **1987**, *27*, 189.

15 A. N. Semenov, *J. Theor. Exp. Phys.* **1985**, *61*, 733.

16 S. T. Milner, T. A. Witten, M. E. Cates, *Macromolecules* **1988**, *21*, 2610.

17 S. T. Milner, T. A. Witten, M. E. Cates, *Europhys. Lett.* **1988**, *5*, 413.

18 S. T. Milner, *Science (80-)* **1991**, *251*, 905.

19 M. Wijmans, E. B. Zhulina, *Macromolecules* **1993**, *26*, 7214.

20 E. K. Lin, A. P. Gast, *Macromolecules* **1996**, *29*, 390.

21 R. C. Ball, J. F. Marko, S. T. Milner, T. A. Witten, *Macromolecules* **1991**, *24*, 693.

22 D. R. M. Williams, G. H. Fredrickson, *Macromolecules* **1992**, *25*, 3561.

23 F. Lo Verso, S. a. Egorov, A. Milchev, K. Binder, *J. Chem. Phys.* **2010**, *133*, 184901.

24 E. Lindberg, C. Elvingson, *J. Chem. Phys.* **2001**, *114*, 6343.

25 H. Orland, M. Schick, *Macromol. Theory Simul.* **1996**, *29*, 713.

26 E. B. Zhulina, V. A. Pryamitsyn, O. V. Borisov, *Polym. Sci. U.S.S.R.* **1989**, *31*, 205.

27 K. Binder, A. Milchev, *J. Polym. Sci. Part B: Polym. Phys.* **2012**, *50*, 1515.

28 N. Dan, M. Tirrell, *Macromolecules* **1992**, *25*, 2890.

29 Matsen, M. W. In *Soft Matter, Volume 1: Polymer Melts and Mixtures*; G. Gompper, M. Schick, Eds.; Wiley-VCH: Weinheim, **2006**; Vol. *1*, pp 87–178.

30 C. M. Wijmans, J. M. H. M. Scheutjens, E. B. Zhulina, *Macromolecules* **1992**, *25*, 2657.

31 G. Fredrickson, *The Equilibrium Theory of Inhomogeneous Polymers*; Oxford University Press: Oxford, **2005**.

32 J. Schmelz, M. Karg, T. Hellweg, H. Schmalz, *ACS Nano* **2011**, *5*, 9523.

33 D. Richter, D. Schneiders, M. Monkenbusch, L. Willner, L. J. Fetters, J. S. Huang, M. Lin, K. Mortensen, B. Farago, *Macromolecules* **1997**, *30*, 1053.

34 J. Wang, W. Zhu, B. Peng, Y. Chen, *Polymer (Guildf)* **2013**, *54*, 6760.

35 I. A. Zucchi, W. F. Schroeder, *Polym (UK)* **2015**, *56*, 300.

36 E. Raphael, P. G. de Gennes, *Macromol. Chem. Macromol. Symp.* **1992**, *62*, 1.

37 N. A. Gross, E. B. Zhulina, A. C. Balazs, *J. Chem. Phys.* **1996**, *104*, 727.

38 T. A. Vilgis, *Phys. Chem. Chem. Phys.* **1999**, *1*, 2077.

39 R. R. Netz, M. Schick, *Europhys. Lett.* **1997**, *38*, 37.

40 H. Xi, S. T. Milner, *Macromolecules* **1996**, *29*, 4772.